Desulfurization Reactions on $Ni_2P(001)$ and α-$Mo_2C(001)$ Surfaces: Complex Role of P and C Sites

Ping Liu,[†] José A. Rodriguez,*[,†] Takeshi Asakura,[‡] João Gomes,[§] and Kenichi Nakamura[‡]

Department of Chemistry, Brookhaven National Laboratory, Building 555, Upton, New York 11973, Materials and Structures Laboratory, Tokyo Institute of Technology, Yokohama 226-8503, Japan, and IFIMUP, Universidade do Porto, 4169 Porto, Portugal

Received: December 14, 2004

X-ray photoelectron spectroscopy and first-principles density-functional calculations were used to study the interaction of thiophene, H_2S, and S_2 with $Ni_2P(001)$, α-$Mo_2C(001)$, and polycrystalline MoC. In general, the reactivity of the surfaces increases following the sequence MoC < $Ni_2P(001)$ < α-$Mo_2C(001)$. At 300 K, thiophene does not adsorb on MoC. In contrast, $Ni_2P(001)$ and α-$Mo_2C(001)$ can dissociate the molecule easily. The key to establish a catalytic cycle for desulfurization is in the removal of the decomposition products of thiophene (C_xH_y fragments and S) from these surfaces. Our experimental and theoretical studies indicate that the rate-determining step in a hydrodesulfurization (HDS) process is the transformation of adsorbed sulfur into gaseous H_2S. Ni_2P is a better catalyst for HDS than Mo_2C or MoC. The P sites in the phosphide play a complex and important role. First, the formation of Ni−P bonds produces a weak "ligand effect" (minor stabilization of the Ni 3d levels and a small Ni → P charge transfer) that allows a high activity for the dissociation of thiophene and molecular hydrogen. Second, the number of active Ni sites present in the surface decreases due to an "ensemble effect" of P, which prevents the system from deactivation induced by high coverages of strongly bound S. Third, the P sites are not simple spectators and provide moderate bonding to the products of the decomposition of thiophene and the H adatoms necessary for hydrogenation.

I. Introduction

Since the last century petroleum has been a very important source of fossil fuels and chemical feedstocks. Sulfur-containing compounds are common impurities in all crude oil.[1] In our industrial society, these impurities have a negative impact in the processing of oil-derived chemical feedstocks and degrade the quality of the air by forming sulfur oxides (SO_x) during the burning of fuels and by poisoning the catalysts used in vehicle catalytic converters. Hydrodesulfurization (HDS) is one of the largest processes in petroleum refineries where sulfur is removed from the crude oil.[1] Organosulfur compounds are converted to H_2S and hydrocarbons by reaction with hydrogen over a catalyst.[2] Most commercial HDS catalysts contain a mixture of MoS_2 and Ni or Co.[2−4] The current HDS catalysts cannot provide fuels with the low content of sulfur required by new environmental regulations.[2a,5,6] The search for better desulfurization catalysts is a major issue nowadays in industry and academic institutions.[2a,5] Thus, it has been established that β-Mo_2C and other metal carbides are very active for the cleavage of C−S bonds,[7,8] but their HDS activity decreases quickly with time.[9] The degradation of β-Mo_2C has been ascribed to the formation of a chemisorbed layer of sulfur or MoS_xC_y compounds on the surface of the catalyst.[7,9] More recently, transition-metal phosphides have shown a tremendous potential as highly active HDS catalysts.[10−16] Among all the phosphides, Ni_2P/SiO_2 demonstrated the highest HDS activity (HDS conversion of 99%) and has been reported to be more efficient than NiMoS/Al_2O_3 (HDS conversion of 76%).[11,12,14] Furthermore, Ni_2P does not deactivate with time as β-Mo_2C does.[13]

At an atomic level, it is not well understood how nickel phosphide catalysts carry out HDS reactions. Very little is known about the chemical properties of surfaces of Ni_2P or other metal phosphides.[10,12,14,17] In accordance with Sabatier's principle,[17,18] a volcano trend between the HDS activity of a catalyst and metal−sulfur bond strengths has been identified.[6] Pure transition metals are too reactive to be useful as HDS catalysts, being poisoned by strongly bound S adatoms.[1b,2a] The inclusion of P into the lattice of a transition metal produces a substantial gain in stability and moderates the chemical reactivity.[17] In general, the catalytic properties of metal phosphides have been explained in terms of a special electronic structure induced by the presence of phosphorus (a "ligand effect" on the metal)[9,11,12,17] or variations in the number of metal atoms that are exposed in the surface (an "ensemble effect").[10−14] Thiophene is quite reactive on Ni_2P/SiO_2 catalysts.[12b] It is usually assumed that the P atoms in the surface of the catalysts are simple spectators and do not participate directly in desulfurization reactions,[11,13] although P sites are able to bind CO well.[14b]

In this paper we use X-ray photoelectron spectroscopy (XPS) and first-principles density-functional theory (DFT) calculations to investigate the desulfurization of thiophene (a typical test molecule in HDS studies)[2,11,12b,13] and the removal of S on surfaces of Ni_2P, Mo_2C, and MoC. The $Ni_2P(001)$ surface studied in this work, Figure 1, exposes Ni and P sites.[10] This surface is of great relevance because it is the predominant orientation observed in HDS catalysts containing Ni_2P crystallites on a silica support.[12] It has well-defined ensembles of three metal atoms that are separated by ∼3.8 Å.[10] In contrast, an α-$Mo_2C(001)$ surface exposes only metal atoms (Figure 1b).[19]

* To whom correspondence should be addressed. E-mail: rodrigez@bnl.gov. Fax: (631) 344-5815.
[†] Brookhaven National Laboratory.
[‡] Tokyo Institute of Technology.
[§] Universidade do Porto.

10.1021/jp044301x CCC: $30.25
Published on Web 02/18/2005

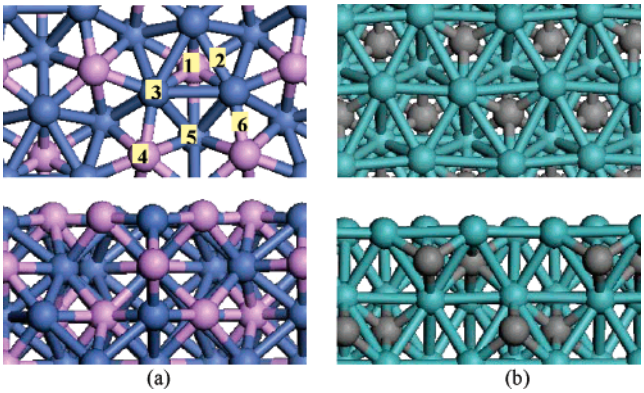

Figure 1. Relaxed structures for $Ni_2P(001)$ (a) and α-$Mo_2C(001)$ (b) surfaces (Mo, cyan; Ni, blue; P, purple; C, gray): top, top view; bottom, side view. The labels in (b) indicate different adsorption sites (1, 3-fold Ni hollow; 2, Ni−Ni bridge; 3, Ni atop; 4, P atop; 5, hybrid hollow sites constructed by three Ni atoms and two P atoms; 6, Ni−P hybrid bridge).

This carbide surface is expected to have a chemical reactivity very similar to that of a metal surface.[19,20] Our results show clear differences in the behavior of sulfur adatoms on Ni_2P-(001) and α-$Mo_2C(001)$. The nature of the metal−sulfur interactions on $Ni_2P(001)$ depends strongly on coverage, and the P atoms are not simple spectators playing a complex and important role in HDS processes.

II. Experimental and Theoretical Methods

II.1. Experimental Studies. The XPS data presented in section III were collected in a conventional ultra-high-vacuum (UHV) chamber (base pressure $\sim 1 \times 10^{-10}$ Torr) equipped with instrumentation for XPS, low-energy electron diffraction (LEED), Auger electron spectroscopy (AES), and temperature-programmed desorption (TPD).[21] The $Ni_2P(001)$, α-$Mo_2C(001)$, and MoC samples were mounted in a manipulator that allowed cooling to 100 K, resistive heating to 1400 K, and e-beam heating to 2500 K.[21]

The clean $Ni_2P(001)$ surfaces were prepared following a procedure similar to that reported in ref 10. Ion bombardment and annealing in UHV at 750 K produced ordered (1×1) hexagonal surfaces that have a composition close to that expected for bulk Ni_2P.[10] Ion bombardment with Ar^+ at 300 K removed surface impurities such as C and S plus P atoms, producing Ni-rich surfaces. Surfaces with the correct stoichiometry were produced by annealing in UHV at temperatures above 700 K (diffusion of P from the bulk to the surface)[10] or by reaction with small amounts of PH_3 gas at 500−600 K. Along the (001) direction of bulk Ni_2P, there is an alternation of planes that have Ni_3P and Ni_3P_2 compositions.[10] A two-plane repeat unit along the (001) direction gives the bulk Ni_2P stoichiometry. LEED and scanning tunneling microscopy (STM) showed that the $Ni_2P(001)$ surfaces used in this study exposed Ni_3P_2 planes (see Figure 1a).[22] DFT calculations indicate that this termination has a lower surface free energy than a Ni_3P termination.

Ion bombardment and subsequent annealing at 1000 K were used to clean and prepare Mo-terminated α-$Mo_2C(001)$ surfaces (Figure 1b).[23] STM images indicate that under these conditions the surfaces have the expected bulk-terminated (1×1) orthorhombic periodicity,[23] with two or three rotationally misaligned orthorhombic domains. The surfaces of MoC investigated in this study are best described as polycrystalline. Surface impurities were removed by Ar^+ sputtering, and a C/Mo ratio close to 1 was restored by exposing the surfaces to C_2H_2 or C_2H_4 at 800−900 K.[7,8b] Several attempts were made to prepare well-defined surfaces of δ-MoC oriented along the (001) plane of this carbide. An ideal δ-MoC(001) surface has a cubic rocksalt structure exposing an equal number of Mo and C atoms.[19,20] The preparation of this particular surface is very difficult due to the complex phase diagram of MoC.[8b,17]

Thiophene and H_2S were dosed to the phosphide and carbide surfaces at 100 or 300 K using capillary dosers. The reported exposures are uncorrected for enhancement factors. Very high coverages of sulfur were obtained by direct dosing of S_2 under UHV conditions. S_2 gas was generated in situ from decomposition of silver sulfide in a solid-state electrochemical cell, Pt/Ag/AgI/Ag_2S/Pt.[21a] Attached to the UHV chamber was a high-pressure cell that was used to expose the sulfided samples to moderate pressures of H_2 (100−500 Torr). After reaction with H_2, the gases were pumped out and the samples were returned to the UHV chamber for surface characterization.

II.2. Theoretical Studies. The DFT calculations reported in section III were performed using the CASTEP (Cambridge Serial Total Energy Package) suite of programs,[24] which have proved to be very useful in theoretical studies dealing with metal phosphide and carbide surfaces.[17,19−21] The Kohn−Sham one-electron equations were solved on a basis set of plane waves with kinetic energy below 25 Ry, and ultrasoft pseudopotentials were used to describe the ionic cores.[25] Brillouin zone integration was approximated by a sum over special *k*-points selected using the Monkhorst−Pack scheme.[26] Enough *k*-points (25 or 20) were chosen to make sure that there was no significant change in the calculated energies when a larger number of *k*-points was used. The exchange-correlation energy and the potential were described by the revised version of the Perdew−Burke−Ernzerhof (RPBE) functional.[27] Previous DFT calculations using the RPBE functional predicted adsorption energies for CO, S, SO_2, and thiophene on metal and metal carbide surfaces were very close to those measured experimentally ($|\Delta E| < 0.25$ eV).[19,20,28]

To model the $Ni_2P(001)$ and α-$Mo_2C(001)$ surfaces, Figure 1, we used four-layer slabs[17,19−21] repeated in a supercell geometry with an 11 Å vacuum between the slabs. The interaction of the surfaces with the adsorbates (sulfur and hydrogen) at different coverages was investigated. The surfaces were represented by $\sqrt{3} \times \sqrt{3}$ (for $Ni_2P(001)$) or 2×2 (for α-$Mo_2C(001)$) unit cells with three or four metal atoms in each layer (Figure 1). In the calculations, the top three layers were allowed to relax in all dimensions together with the adsorbates, while the bottom layer was kept fixed at the calculated bulk positions. For each optimized structure, a Mulliken population analysis[29,30] was carried out to estimate the partial charge on each atom and examine *qualitative trends* in charge redistribution.

III. Results and Discussion

In a typical HDS process,[2a,5] organosulfur molecules and H_2 are adsorbed on the surface of a catalyst, then C−S bonds crack apart, and in the final steps the produced S adatoms and C_xH_y fragments are hydrogenated and desorb into the gas phase. Thiophene (C_4H_4S) is a common test molecule used in HDS studies.[2,11,12b,13] This section is organized as follows. First, we investigate the interaction of C_4H_4S, H_2S, and S_2 with the phosphide and carbide surfaces using XPS. The focus is on the cleavage of C−S bonds and the subsequent reaction of the S adatoms and C_xH_y with H_2 gas. At the end of this section, DFT calculations are used to study the nature of the bonding of S to $Ni_2P(001)$ and α-$Mo_2C(001)$, and the energetics for the HDS of thiophene.

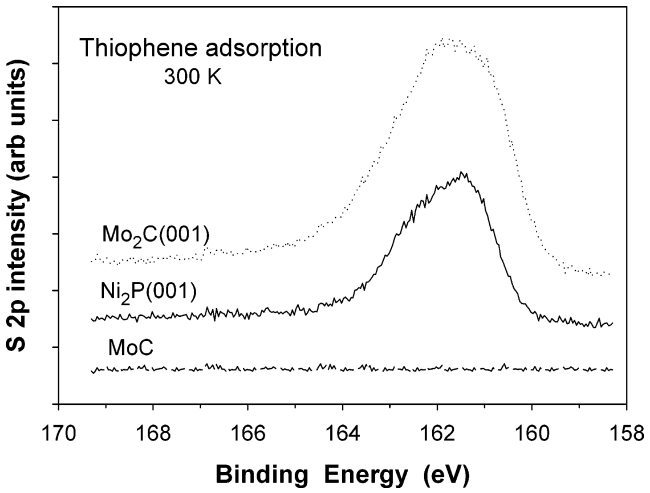

Figure 2. S 2p XPS spectra recorded after a saturation dose of thiophene (2 langmuirs) was given to $Ni_2P(001)$, α-$Mo_2C(001)$, and polycrystalline MoC at 300 K.

III.1. Reaction with Thiophene: XPS Studies. C_4H_4S was dosed to the $Ni_2P(001)$, α-$Mo_2C(001)$, and MoC surfaces at 100 or 300 K. Figure 2 shows S 2p XPS spectra acquired after the molecule (2 langmuirs) was dosed at room temperature. For chemisorbed thiophene, the S 2p features are expected at 167−164 eV.[7a] The position of the S 2p features seen for the C_4H_4S/$Ni_2P(001)$ and C_4H_4S/α-$Mo_2C(001)$ systems, 164−160 eV, is typical of sulfur adatoms,[7,21a] indicating cleavage of the C−S bonds in thiophene. In contrast, the molecule does not dissociate or adsorb on MoC at 300 K.

Two previous studies have examined the interaction of thiophene with α-$Mo_2C(001)$.[20,30] Photoemission results indicate that C−S bond scission occurs by 170 K and possibly as low as 105 K upon adsorption.[30] DFT calculations also observe a very strong interaction between C_4H_4S and α-$Mo_2C(001)$.[20] The molecule adsorbs with its ring parallel to the carbide surface, and one of the C−S bonds spontaneously breaks.[20] The α-$Mo_2C(001)$ surface exhibits a reactivity similar to that found for surfaces of pure Mo[7a,19,31,32] on which the cleavage of the C−S bonds in C_4H_4S is not a problem.

Theoretical studies have shown weak bonding interactions for thiophene on a flat δ-MoC(001) surface.[20] A Mo → C charge transfer (ligand effect) and a dilution in the fraction of metal atoms in the surface (ensemble effect) make δ-MoC(001) inert toward thiophene.[20] Our experimental results for C_4H_4S/MoC confirm this theoretical prediction. We found that thiophene adsorbs on polycrystalline MoC at 100 K, and desorbs intact upon heating to 200 K. From our TPD experiments, we estimate a thiophene adsorption energy of ∼11 kcal/mol (0.48 eV),[33] which is close to the value of 7 kcal/mol (0.3 eV) calculated for C_4H_4S on a flat δ-MoC(001) surface.[20]

In the case of $Ni_2P(001)$, the Ni → P charge transfer is not large (<0.1 e)[13,17] and the surface has a substantial number of Ni atoms. Clusters of three Ni atoms are present (Figure 1a), and the separation between these clusters (∼3.8 Å) is not large enough to prevent effective bonding interactions with a relatively big molecule such as thiophene. At 100 K we found molecular adsorption of C_4H_4S on $Ni_2P(001)$, but at temperatures above 200 K the surface was able to crack the C−S bonds of the adsorbate. Similar results have been found for the interaction of thiophene with Ni_2P/SiO_2 catalysts.[12c]

Thus, it is clear that α-$Mo_2C(001)$ and $Ni_2P(001)$ can dissociate thiophene easily. The key to establish a catalytic cycle for desulfurization is in the removal of the decomposition products of thiophene (C_xH_y fragments and S) from these surfaces. Figure 3 shows XPS data for the cleaning by reaction with H_2 (500 Torr) of a $Ni_2P(001)$ surface that was exposed to a saturation coverage of thiophene at 300 K (Figure 2). HDS reactions on nickel phosphide catalysts are fast at temperatures above 600 K.[10−16] At a temperature of 450 K, we found that it was possible to hydrogenate and remove the C_xH_y fragments present on the $Ni_2P(001)$ surface. On the other hand, the removal of the S adatoms ($S_{ads} + H_{2,gas} \rightarrow H_2S_{gas}$) was significant only at temperatures above 600 K. Arrhenius plots obtained after the hydrogenation rates were measured at different temperatures (450, 500, 600, and 650 K) gave *apparent* activation energies of 19−21 kcal/mol (0.8−0.9 eV) for the removal of S and 7−9 kcal/mol (0.3−0.4 eV) for the removal of the C_xH_y fragments. When similar experiments were done for the α-$Mo_2C(001)$ surface, again we found that the most difficult step in an HDS process should be the transformation of adsorbed sulfur into gaseous H_2S. In fact, at a temperature of 650 K, we were unable to remove most (∼89%) of the S adsorbed on α-$Mo_2C(001)$. In the rest of the paper, we will focus on the interaction of H_2S and S with the carbide and phosphide surfaces.

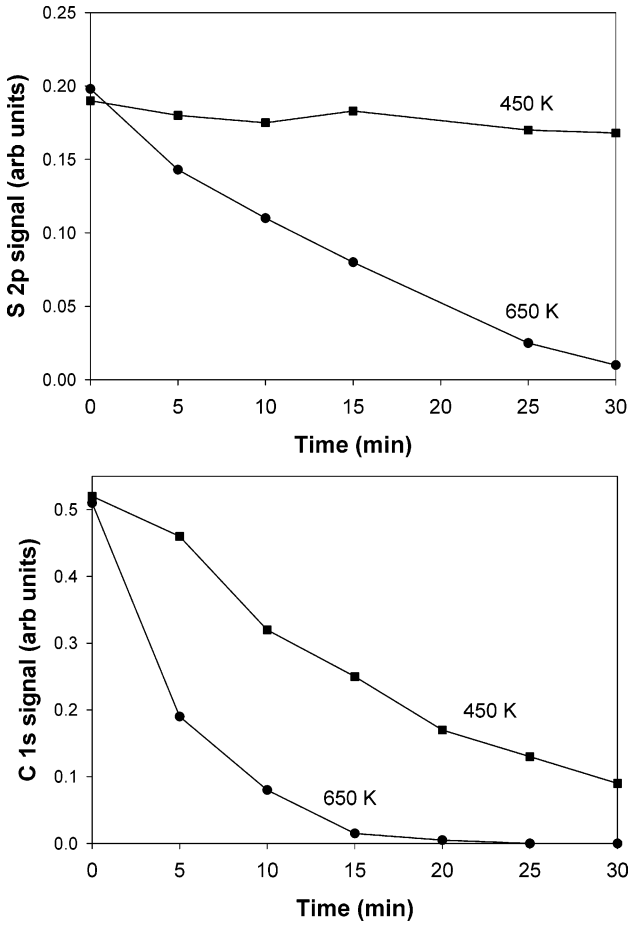

Figure 3. Hydrogenation of S adatoms and C_xH_y fragments produced by the decomposition of thiophene on $Ni_2P(001)$. Initially, the phosphide surface was exposed to a saturation dose of thiophene (2 langmuirs) at 300 K. Then, the sample was transferred from the UHV chamber into a high-pressure cell for reaction with H_2 (500 Torr) at 450 or 650 K. The removal of S and C_xH_y was followed by measuring the changes in the S 2p and C 1s XPS signals as a function of reaction time.

III.2. Reaction with H_2S and S_2: XPS Studies. Figure 4 shows the uptake of sulfur after H_2S was dosed to $Ni_2P(001)$, α-$Mo_2C(001)$, and MoC surfaces at 300 K. The reactivity of the surfaces toward H_2S increases following the sequence MoC < $Ni_2P(001)$ ≪ α-$Mo_2C(001)$. MoC probably has a low

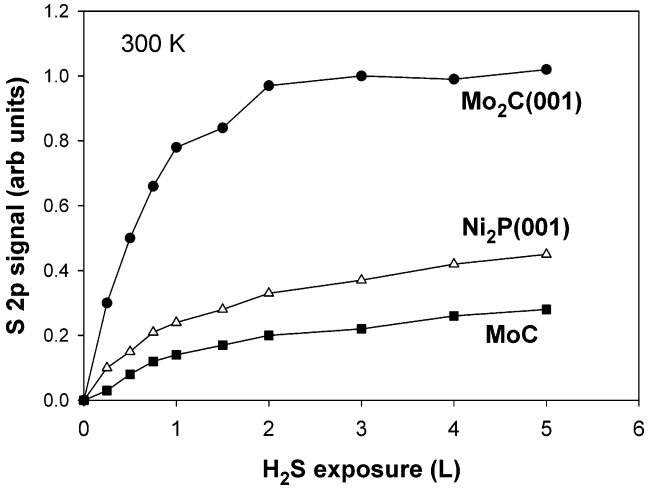

Figure 4. Uptake of sulfur after H_2S was dosed to $Ni_2P(001)$, α-Mo_2C-(001), and polycrystalline MoC at 300 K.

reactivity toward H_2S due to a large Mo → C charge transfer (ligand effect) that passivates the metal centers.[19,20] In the following section we will see that the relative rates of H_2S dissociation (slopes in the curves of Figure 4) reflect trends in the strength of the H_2S ↔ $Ni_2P(001)$ and H_2S ↔ $Mo_2C(001)$ bonding interactions.

We found that S_2 was more efficient than H_2S to generate large coverages of sulfur on the phosphide and carbide surfaces under UHV conditions. As the sulfur coverage increases, the dissociation of H_2S becomes difficult under UHV.[1b] Figure 5 shows S 2p spectra taken after given saturation doses of H_2S and S_2 to a $Ni_2P(001)$ surface at 300 K. A doublet of peaks, at 164−160 eV, is seen after saturation with H_2S. This feature was also seen for small doses of S_2, but the S 2p spectrum became more complex at higher coverages of sulfur (middle of Figure 5). The S 2p spectrum for a surface saturated with S_2 was well fitted[21a] by a set of two doublets, appearing at 165−162 and 164−160 eV. When the sulfur coverage rose, there was a clear change in the strength of the bonding interactions between the adsorbate and surface. The sulfur adatoms produced by the dissociation of H_2S or after small doses of S_2 were strongly bound and remained on the phosphide surface upon annealing to temperatures as high as 700 K. In contrast, the sulfur species that produced the S 2p features at higher binding energy in Figure 4 (165−162 eV) desorbed upon heating to 400−450 K. This "weakly" bound sulfur could be attached to Ni *and/or* P sites, since it induced a significant change in the line shape of the P 2p XPS spectrum for the phosphide substrate. It is known that the P atoms in Ni_2P/SiO_2 catalysts can bind CO molecules.[14b]

The α-$Mo_2C(001)$ surface bonds strongly small and large coverages of sulfur. The final sulfur coverage seen in Figure 4 after large doses of H_2S, characterized by one doublet at 164−160 eV in S 2p XPS spectra, did not change when the sample was heated to 700 K. Figure 6 compares the rates for removal of moderate to small coverages of S from $Ni_2P(001)$ and α-$Mo_2C(001)$. Initially, approximately the same amount of sulfur (S 2p intensity of 0.4 in Figure 4) was deposited on both surfaces, and then they were exposed to H_2 (500 Torr) at high temperature (650 K). The $H_{2,gas} + S_{ads} \rightarrow H_2S_{gas}$ reaction proceeds faster on $Ni_2P(001)$. In fact, only a very small amount of sulfur is removed from α-$Mo_2C(001)$. The DFT calculations shown below indicate that this is a direct consequence of very strong S−$Mo_2C(001)$ bonds.

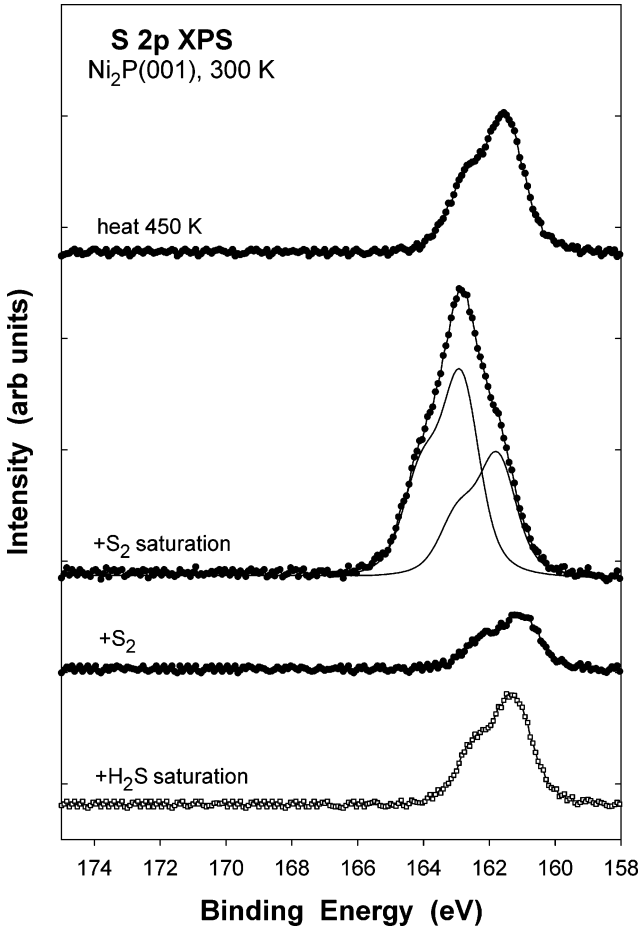

Figure 5. S 2p XPS spectra taken after given saturation doses of H_2S (□) and S_2 (●) to a $Ni_2P(001)$ surface at 300 K.

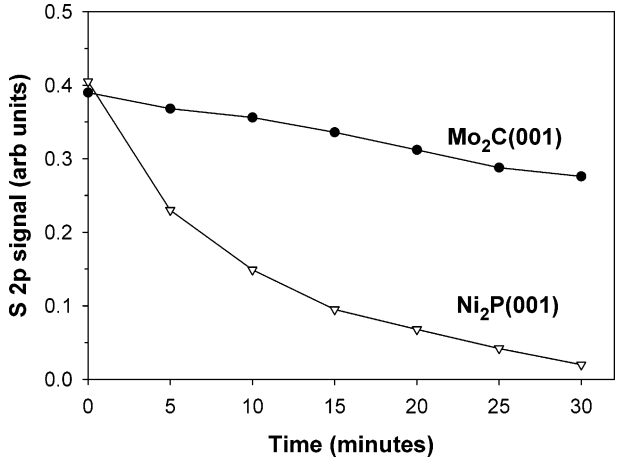

Figure 6. Hydrogenation of S adatoms produced by the decomposition of H_2S on $Ni_2P(001)$ and α-$Mo_2C(001)$ at 300 K. Initially, approximately the same amount of sulfur (S 2p intensity of 0.4 in Figure 4) was deposited on both surfaces. Then, the samples were transferred from the UHV chamber into a high-pressure cell for reaction with H_2 (500 Torr) at 650 K. The removal of S was followed by measuring the changes in the S 2p XPS signal as a function of reaction time.

III.3. Bonding of Sulfur to $Ni_2P(001)$ and α-$Mo_2C(001)$: DFT Studies. Here, we use DFT calculations to examine the nature of the bonding between sulfur and $Ni_2P(001)$ or α-Mo_2C-(001) surfaces. To start, a geometry optimization was first carried out. Bulk Ni_2P adopts a hexagonal structure.[10,34] An orthorhombic structure was considered for bulk α-Mo_2C.[35] The optimized structural parameters for the bulk materials were in

TABLE 1: DFT-Optimized Lattice Parameters

		lattice constant (Å)		
	cryst syst	*a*	*b*	*c*
Ni_2P	hexagonal	5.93 (5.87[34])	5.93 (5.87[34])	3.37 (3.39[34])
α-Mo_2C	orthorhombic	4.82 (4.73[35])	6.01 (6.03[35])	5.15 (5.20[35])

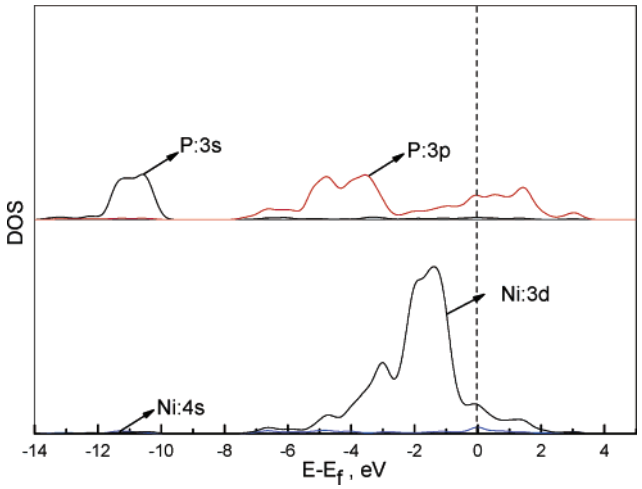

Figure 7. Projected local density of states (LDOS) for the Ni(4s,4d) and P(3s,3p) states of the Ni_3P_2-terminated $Ni_2P(001)$ surface.

good agreement with the experimental values (differences in lattice constant <0.2 Å; see Table 1). Along the [001] direction of Ni_2P, Ni_3P and Ni_3P_2 planes alternate to give the full stoichiometry of the bulk (Figure 1a).[10,12] In our DFT calculations, the Ni_3P_2-terminated surface was found to be more stable than a Ni_3P-terminated surface by 2.75 eV/unit cell. This is consistent with the results of LEED and STM studies for Ni_2P-(001).[22] The DFT studies also indicate that the bonds in Ni_2P-(001) are covalent in nature. Although the s and d orbitals of Ni are mixed with the s and p orbitals of P as shown in Figure 7, the valence bands in $Ni_2P(001)$ exhibit strong metal d character, and the Ni atoms and P atoms of the surface are slightly charged (Ni, 0.07e; P, −0.07e). Previous experimental studies also point to a metallic behavior for Ni_2P.[10,12,13,36] Valence photoemission spectra for $Ni_2P(001)$[10] show a valence band in which the Ni 3d levels mainly appear at 1−3 eV below the Fermi edge, as seen in the DOS plot of Figure 7.

The geometry of an α-$Mo_2C(001)$ surface has been extensively investigated in both theory and experiment.[19,20,23] A Mo-terminated (001) plane was used here to describe the surface of Mo_2C, which includes alternating Mo and C layers (Figure 1b). Mo atoms in the surface of Mo_2C have been found to be as reactive as those of pure Mo with only ~0.3e transferring to the C atoms in the subsurface.[19,20]

To understand better the experimental data in Figure 4, we calculated the energy change associated with the dissociative adsorption of hydrogen sulfide ($H_2S_{gas} \rightarrow S_{ads} + H_{2,gas}$) on Ni_2P-(001) and α-$Mo_2C(001)$:

$$E_S = E(n\mathrm{S/Surf}) + nE(H_2) - E(\mathrm{surf}) - nE(H_2S) \quad (1)$$

where *n* is the number of S atoms adsorbed per unit cell. The driving force for this reaction is the formation of bonds between S and the phosphide or carbide surface. Figure 8a displays the optimized geometries for S adsorption on the surfaces at different coverages, and the corresponding energies (E_S) are shown in Figure 8b.

For a coverage of 0.33 monolayer (ML) of S on the Ni_2P-(001) surface (the smallest S coverage that we were able to calculate for this system), the adsorbate preferred to sit on the Ni hollow sites (1 in Figure 1a) with a bonding energy of −1.28 eV (E_S, Figure 8b). At this coverage, the S adsorption on the Ni bridge (2 in Figure 1a) or Ni atop (3 in Figure 1a) sites, as well as on hybrid hollow sites constructed by two P atoms and three Ni atoms (5 in Figure 1a), was not stable and the adatom spontaneously moved to the Ni hollow sites (Figure 8a). S bonded to these sites probably yielded the doublet of peaks seen in S 2p XPS spectra after H_2S or small amounts of S_2 were dosed to the $Ni_2P(001)$ substrate (Figure 5). At S coverages of 0.67 and 1 ML, all the Ni hollow sites are saturated with a fraction of the adsorbed S and the other S atoms favor Ni−P bridge sites (Figure 8a). When the S coverage increases, E_S in Figure 8b varies from −1.28 eV (θ_S = 0.33 ML) to −0.64 eV (θ_S = 0.67 ML), and finally to 0.67 eV (θ_S = 1.0 ML). Thus, the production of high coverages of S by the dissociation of H_2S under UHV conditions is difficult. The DFT results in Figure 8 correlate well with the trends seen for the S 2p XPS spectra in Figure 5. Both indicate that there are two kinds of sites for S adsorption on $Ni_2P(001)$. One is the Ni hollow site that is populated at low S coverage and leads to a strong adsorption bond. The other is a Ni−P bridge site that is probably populated at medium or large coverages and does not interact with S strongly. This adsorption site is interesting since it allows the participation of P atoms in HDS reactions.

The DFT calculations indicate that α-$Mo_2C(001)$ is very reactive toward H_2S or sulfur. On this surface, the S atoms always adsorb at 3-fold Mo sites. In Figure 8b, E_S becomes more and more exothermic when the S coverage on α-Mo_2C-(001) increases from 0.25 to 1 ML. This can be seen as the prelude to the formation of a MoC_xS_y compound.[9] Only when the S coverage reaches 1.25 or 1.5 MLs, there is a weakening of the bonding interactions of the adsorbate with the surface. At this point, the extra S atoms do not occupy the Mo 3-fold sites, but react with the adsorbed sulfur atoms, forming S_2 (Figure 8a) or S_4 clusters, a phenomenon also observed in experiments for S/Mo(110).[37] In Figure 8, the variation of E_S as a function of S coverage is quite different in the cases of $Ni_2P(001)$ and α-$Mo_2C(001)$. Such a big difference in behavior can have a very important effect on the HDS activity of these materials.

III.4. Thiophene Hydrodesulfurization on $Ni_2P(001)$ and α-$Mo_2C(001)$: DFT Studies. In a typical HDS process, thiophene reacts with hydrogen to be converted into butadiene and H_2S.[1] The exact mechanism for the adsorption of C_4H_4S and the cleavage of its C−S bonds can be very complex.[2a,5a,7,11,20,30−32,34] DFT calculations and photoemission have been used previously to study this mechanism in detail on α-$Mo_2C(001)$.[20,30] On the basis of this and our experimental results in section III.1, we assume that the HDS of thiophene can be divided into two basic sets of reactions: C_4H_4S decomposition and hydrogenation to produce adsorbed sulfur (S_{ads}) and butadiene (C_4H_6)

$$C_4H_4S(g) + H_2(g) \rightarrow S_{ads} + C_4H_6(g) \quad (2)$$

and the removal of adsorbed sulfur in the form of gaseous H_2S

$$S_{ads} + H_2(g) \rightarrow H_2S(g) \quad (3)$$

The whole HDS cycle is exothermic (−0.27 eV). Thus, the conversion is inhibited by kinetics. As shown in reactions 2 and 3, S_{ads} is a key intermediate. Following Sabatier's principle,[17,18] good HDS catalysts should be those that are inert enough to easily remove the adsorbed sulfur, but still able to

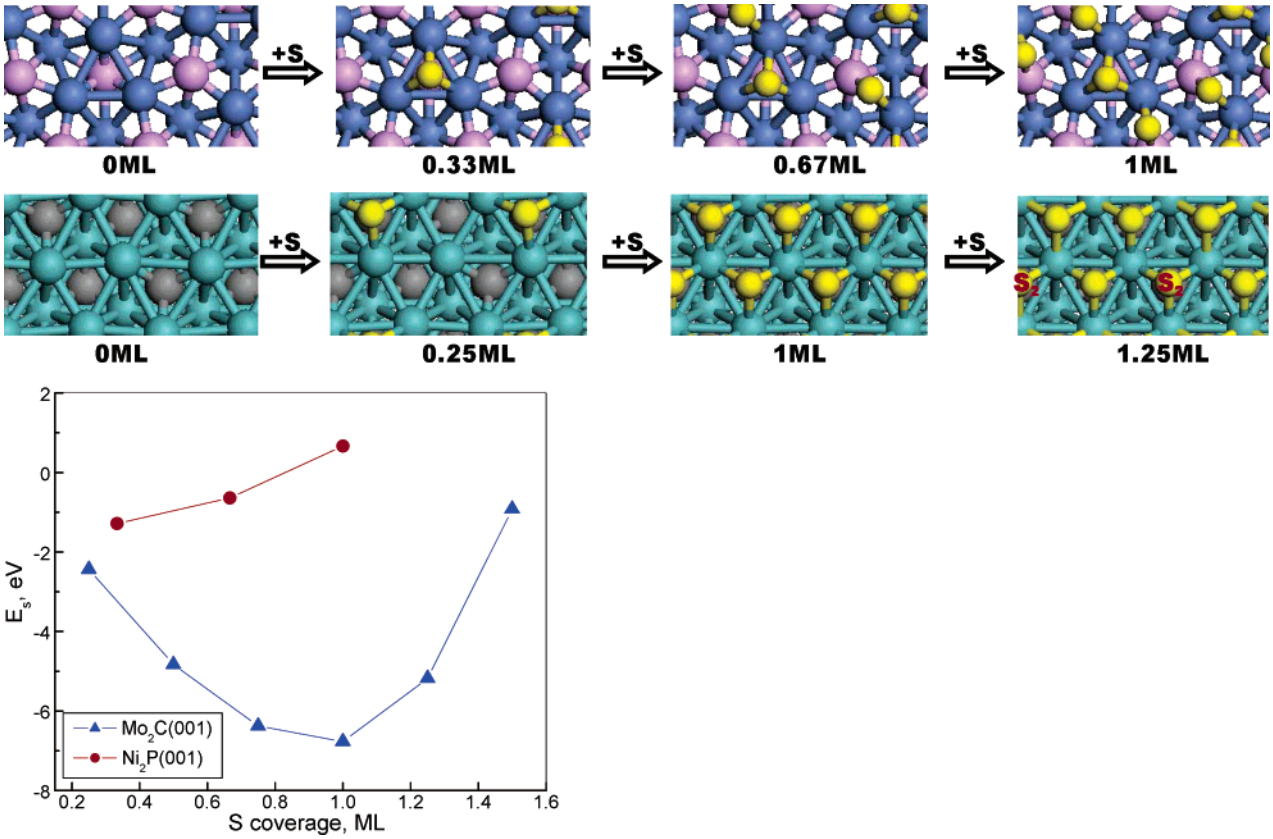

Figure 8. Bonding of the sulfur produced by the $H_2S(gas) \rightarrow S(ads) + H_2(gas)$ reaction on $Ni_2P(001)$ and α-$Mo_2C(001)$ surfaces (Mo, cyan; Ni, blue; P, purple; S, yellow; C, gray): (a, top) optimized structures (top view) at a given coverage, (b, bottom) corresponding bonding energies for sulfur, E_S, in eq 1.

dissociate thiophene and molecular hydrogen. The XPS studies have shown above that both $Ni_2P(001)$ and α-$Mo_2C(001)$ can easily dissociate thiophene.

Figure 9 summarizes the DFT results for reaction 3 on Ni_2P-(001) and α-$Mo_2C(001)$, including the intermediates involved in each step (Figure 9a) and the calculated potential energy diagram for the reaction (Figure 9b). The energies shown in the figure are relative to those of the clean surface and a free H_2S molecule in the gas phase. The reaction starts with an adsorbed S adatom and a free H_2 molecule ($S_{ads} + H_2(g)$), followed by dissociation of H_2 ($S_{ads} + 2H_{ads}$*), migration of H adatoms ($S_{ads} + 2H_{ads}$), and formation and removal of H_2S. As shown in Figures 6 and 9, both the experimental data and DFT calculations indicate that the hydrogenation and removal of S adatoms is an endothermic or uphill process, and it is much easier on Ni_2P than on Mo_2C ($\Delta E = 1.28$ eV for Ni_2P and 2.45 eV for Mo_2C). On the $Ni_2P(001)$ surface, a H_2 molecule first dissociates on the Ni hollow sites which are not occupied by the sulfur (H_{ads}*, Figure 9a). This is a downhill reaction, with the energy decreasing by 1.07 eV ($S_{ads} + 2H_{ads}$*, Figure 9). To form H_2S, the H adatoms migrate to the P sites close to the sulfur adsorbed at the Ni hollow sites ($S_{ads} + 2H_{ads}$, Figure 9) with an energy cost of 1.53 eV. Then, an adsorbed HS intermediate is formed. The final step is the desorption of H_2S ($H_2S(g)$, Figure 9), which is also an endothermic process, and the energy increases further by 0.81 eV. In comparison, removing sulfur from α-$Mo_2C(001)$ is much more difficult. As shown in Figure 9b, similar to the case of Ni_2P, the dissociation of H_2 on α-$Mo_2C(001)$ is an exothermic step, while the rest are all energy-consuming processes. The reactants as well as the intermediates involved in the hydrogenation process bond much more strongly with Mo_2C than with Ni_2P. As a result, the last step (removal of H_2S from Mo_2C) becomes highly activated with a reaction energy of 3.66 eV, while it is only 0.81 eV in the case of Ni_2P, indicating that the S-poisoning on Mo_2C should be more serious than on Ni_2P. In the DFT calculations of Figure 9, we started with S bound in its most stable configuration on $Ni_2P(001)$. A S bound to a Ni−P bridge site will be much easier to transform into H_2S gas ($\Delta E \approx 0.6$ eV) than a S bound to a Ni hollow site ($\Delta E \approx 1.3$ eV).

Finally, we take a step further to investigate a catalytic cycle of thiophene HDS over a $Ni_2P(001)$ surface. The corresponding energy diagram is presented in Figure 10, where the energies are relative to those of a clean $Ni_2P(001)$ surface, two H_2 molecules, and a thiophene molecule in the gas phase. As expressed in reactions 2 and 3, two processes were considered. Our DFT calculations show that the cleavage of C−S bonds in thiophene and the hydrogenation of C_4H_4 fragments ($2H_2(g) + C_4H_4S(g) \rightarrow S_{ads} + H_2(g) + C_4H_6(g)$) is a highly exothermic process (overall ΔE of −1.89 eV), and eventually provides the energy necessary for the removal of sulfur from the phosphide surface. In accordance with the experimental observations, the removal of the adsorbed S from the surface is the rate-determining step in the HDS of thiophene over $Ni_2P(001)$.

The thiophene HDS on α-$Mo_2C(001)$ is not included in Figure 10. The problem here is that the reactions associated with processes 2 and 3 are very difficult to complete on α-Mo_2C-(001). Our experimental data show that thiophene decomposes on this carbide surface, but the hydrogenation of the S adatoms and C_xH_y fragments is not effective. The XPS results point to the formation of MoC_xS_y compounds that have a Mo/C atomic ratio substantially smaller than 2 (1.4 < Mo/C atomic ratio < 1.7). This is consistent with models that have been proposed for the deactivation of β-Mo_2C HDS catalysts.[5,7,9]

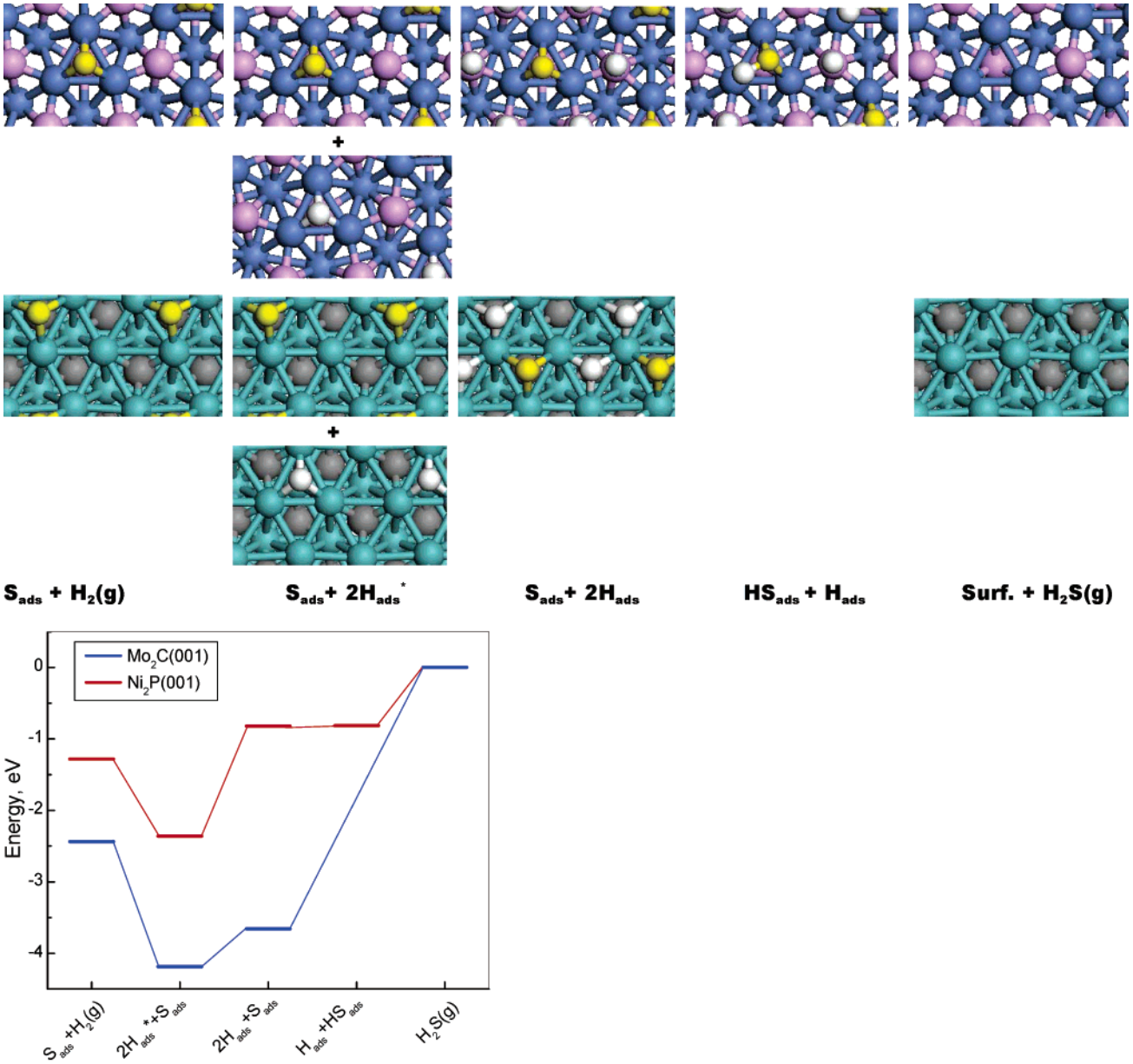

Figure 9. Hydrogenation and removal of sulfur adatoms from $Ni_2P(001)$ and α-$Mo_2C(001)$ surfaces (Mo, cyan; Ni, blue; P, purple; S, yellow, C, gray; H, white): (a, top) optimized structures (top view) for each step of the reaction process; (b, bottom) corresponding energies for each step relative to those of the clean surfaces and a H_2S molecule in the gas phase. "H_{ads}" and "H_{ads}*" correspond to atomic hydrogen adsorbed at the sites close to and away from the adsorbed sulfur atom (S_{ads}), respectively.

According to our results, the very good catalytic performance reported for Ni_2P[11−14] can be ascribed to the effects and behavior of the P sites. First, the ligand effect of P atoms on the Ni sites is relatively weak. The formation of Ni−P bonds produces a minor stabilization of the Ni 3d levels, and the Ni → P charge transfer is very small. This leads to a reasonably high activity of Ni_2P to dissociate thiophene and hydrogen. Second, the active Ni sites of the surface decrease due to an ensemble effect of P, which prevents the system from the deactivation induced by high coverages of strongly bound S. In addition, our DFT results indicate that the P sites play an important role in the bonding of intermediates. When the Ni hollow sites are occupied by an adsorbate, the P sites can provide moderate bonding to the products of the decomposition of thiophene and the H adatoms necessary for hydrogenation. In the case of α-$Mo_2C(001)$, the C atoms underneath the surface also decrease the chemical activity of the exposed Mo atoms by shifting down their d-band position (ligand effect).[19,20] However, the deactivation is not very strong, and the Mo atoms remain with a higher reactivity than Ni atoms in Ni_2P. Furthermore, the adsorption sites of α-$Mo_2C(001)$ contain only metal atoms (no ensemble effect). As a result of this, plenty of sulfur atoms are trapped in the surface and form very stable MoC_xS_y compounds. Even if the α-$Mo_2C(001)$ surface is partly terminated by C, a high activity toward S and S-containing molecules is also expected according to our previous study.[19] In the extreme case of MoC, a big Mo → C charge transfer and a pronounced ensemble effect make this carbide useless for the dissociation of thiophene.[20]

IV. Summary and Conclusions

X-ray photoelectron spectroscopy and first-principles density-functional calculations were used to study the interaction of thiophene, H_2S, and S_2 with $Ni_2P(001)$, α-$Mo_2C(001)$, and

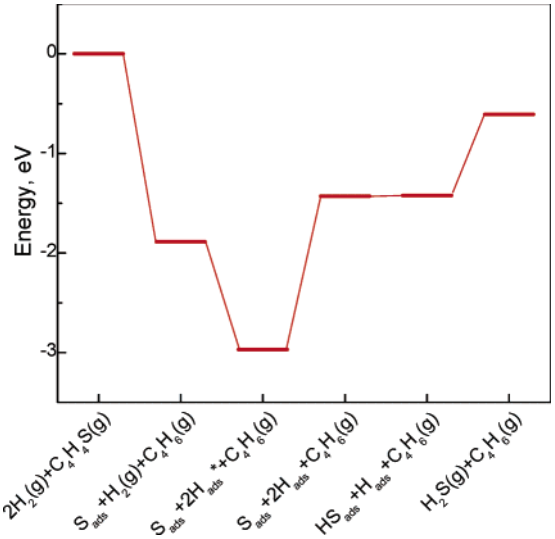

Figure 10. Energy diagram for the catalytic cycle of the HDS of thiophene on a $Ni_2P(001)$ surface. The energies shown in the figure are relative to those of the clean $Ni_2P(001)$ surface, two H_2 molecules, and a thiophene molecule in the gas phase. "H_{ads}" and "H_{ads}*" correspond to atomic hydrogen adsorbed at the sites close to and away from the adsorbed sulfur atom (S_{ads}), respectively.

polycrystalline MoC. In general, the reactivity of the surfaces increases following the sequence MoC < $Ni_2P(001)$ < α-Mo_2C-(001). At 300 K, thiophene does not adsorb on MoC. In contrast, $Ni_2P(001)$ and α-$Mo_2C(001)$ can dissociate the molecule easily. α-$Mo_2C(001)$ interacts much stronger with S and H_2S than Ni_2P-(001). The key to establish a catalytic cycle for desulfurization is in the removal of the decomposition products of thiophene (C_xH_y fragments and S) from these surfaces. Our experimental and theoretical studies indicate that the rate-determining step in an HDS process is the transformation of adsorbed sulfur into gaseous H_2S. α-$Mo_2C(001)$ interacts much stronger with S and H_2S than $Ni_2P(001)$. On the phosphide surface, there are two adsorption states for sulfur. Sulfur bonded to Ni hollow sites is stable up to temperatures above 700 K, while sulfur bonded to Ni−P bridge sites desorbs in the range of 400−450 K. The bonding energy of S on $Ni_2P(001)$ decreases with increasing coverage. An opposite trend is seen for S/$Mo_2C(001)$, as a consequence of MoC_xS_y compound formation, and large coverages of sulfur remain on the carbide surface after heating to 700 K.

Thus, Ni_2P should be a better catalyst for HDS than Mo_2C or MoC. The P sites of the phosphide play a complex and important role. First, the formation of Ni−P bonds produces a weak ligand effect (minor stabilization of the Ni 3d levels and a small Ni → P charge transfer) that allows a reasonably high activity for the dissociation of thiophene and molecular hydrogen. Second, the number of active Ni sites present in the surface decreases due to an ensemble effect of P, which prevents the system from the deactivation induced by high coverages of S. Third, the P sites are not simple spectators and provide moderate bonding to the products of the decomposition of thiophene and the H adatoms necessary for hydrogenation.

Ni_2P is a highly active HDS catalyst by obeying Sabatier's principle: good bonding with the reactants, and moderate bonding with the products. The carbides Mo_2C and MoC are not as good HDS catalysts because one interacts too strongly with the products (Mo_2C) and the other has problems dissociating the reactants (MoC).

Acknowledgment. The research carried out at Brookhaven National Laboratory was supported by the U.S. Department of Energy, Division of Chemical Sciences, under Contract DE-AC02-98CH10886. J.G. and K.N. thank the Fundação para a Ciência e Tecnologia (Lisbon), the European Union, and the Nippon Foundation for Materials Science for grants that made possible travel between countries and the research carried out in Portugal and Japan.

References and Notes

(1) (a) Speight, J. G. *The Chemistry and Technology of Petroleum*, 2nd ed.; Dekker: New York, 1991. (b) Rodriguez, J. A.; Hrbek, J. *Acc. Chem. Res.* **1999**, *32*, 719. (c) Friend, C. M.; Chen, D. A. *Polyhedron* **1997**, *16*, 3165.

(2) (a) Topsøe, H.; Clausen, B. S.; Massoth, F. E. *Hydrotreating Catalysis*; Springer-Verlag: New York, 1996. (b) Rodriguez, J. A.; Dvorak, J.; Capitano, A. T.; Gabelnick, A. M.; Gland, J. L. *Surf. Sci.* **1999**, *429*, L426. (c) Rodriguez, J. A. *J. Phys. Chem. B* **1997**, *101*, 7524.

(3) Borgna, A.; Hensen, E. J. M.; Veen, van J. A. R.; Niemantsverdriet, J. W. *J. Catal.* **2004**, *221*, 541.

(4) Travert, A.; Nakamura, H.; Santen, van R. A.; Cristol, S.; Paul, J.; Payen, R. *J. Am. Chem. Soc.* **2002**, *124*, 7084.

(5) (a) Furimsky, E. *Appl. Catal., A* **2003**, *240*, 1. (b) Clark, P.; Wang, X.; Oyama, S. T. *J. Catal.* **2002**, *207*, 256.

(6) (a) Jacobsen, C. J. H.; Törnqvist, E.; Topsøe, H. *Catal. Lett.* **1999**, *63*, 179. (b) Chianelli, R. R.; Berhault, G.; Raybaud, P.; Kasztelan, S.; Hafner, J.; Toulhoat, H. *Appl. Catal., A* **2002**, *227*, 83.

(7) (a) Rodriguez, J. A.; Dvorak, J.; Jirsak, T. *Surf. Sci.* **2000**, *457*, L413. (b) Rodriguez, J. A.; Dvorak, J.; Jirsak, T. *J. Phys. Chem. B* **2000**, *104*, 11515.

(8) (a) Schwartz, V.; da Silva, V. T.; Oyama, S. T. *J. Mol. Catal. A* **2000**, *163*, 251. (b) Chen, J. G. *Chem. Rev.* **1996**, *96*, 1447.

(9) (a) Aegerter, P. A.; Quigley, W. W. C.; Simpson, G. J.; Ziegler, D. D.; Logan, J. W.; McCrea, K. R.; Glazier, S.; Bussell, M. E. *J. Catal.* **1996**, *164*, 109. (b) Diaz, B.; Sawhill, S. J.; Bale, D. H.; Main, R.; Phillips, D. C.; Korlann, S.; Self, R.; Bussell, M. E. *Catal. Today* **2003**, *86*, 191.

(10) Kanama, D.; Oyama, S. T.; Otani, S.; Cox, D. F. *Surf. Sci.* **2004**, *552*, 8.

(11) Oyama, S. T. *J. Catal.* **2003**, *216*, 343.

(12) (a) Sawhill, S. J.; Phillips, D. C.; Bussell, M. E. *J. Catal.* **2003**, *215*, 208. (b) Layman, K. A.; Bussell, M. E. *J. Phys. Chem. B* **2004**, *108*, 15791.

(13) Rodriguez, J. A.; Kim. J. Y.; Hanson. J. C.; Sawhill, S. J.; Bussell, M. E. *J. Phys. Chem. B* **2003**, *107*, 6276.

(14) (a) Oyama, S. T.; Wang, X.; Lee, Y. K.; Bando, K.; Requejo, F. G. *J. Catal.* **2002**, *210*, 207. (b) Layman, K. A.; Bussell, M. E. *J. Phys. Chem. B* **2004**, *108*, 15791.

(15) (a) Korányi, T. *Appl. Catal., A* **2002**, *237*, 1. (b) Sun, F.; Wu, W.; Wu, Z.; Guo, J.; Wei, Z.; Yang, Y.; Jiang, Z.; Tian, F.; Li, C. *J. Catal.*, in press.

(16) Stinner, C.; Prins, R.; Weber, T. *J. Catal.* **2001**, *202*, 187.

(17) Liu, P.; Rodriguez, J. A. *Catal. Lett.* **2003**, *91*, 247.

(18) (a) Sabatier, P. *Ber. Dtsch. Chem. Ges.* **1911**, *44*, 2001. (b) Boudart, M. Djèga-Mariadassou, G. In *Kinetics of Heterogeneous Catalytic Reactions*; Princeton University Press: New York, 1984. (c) Nørskov, J. K.; Bligaard, T.; Logadottir, A.; Bahn, S.; Hansen, L. B.; Bollinger, M.; Bengaard, H.; Hammer, B.; Sljivancanin, Z.; Mavrikakis, M.; Xu, Y.; Dahl, S.; Jacobsen, C. J. H. *J. Catal.* **2002**, *209*, 275.

(19) Liu, P.; Rodriguez, J. A. *J. Chem. Phys.* **2004**, *120*, 5414.

(20) Liu, P.; Rodriguez, J. A.; Muckerman, J. T. *J. Phys. Chem. B* **2004**, *108*, 15662.

(21) (a) Rodriguez, J. A.; Liu, P.; Dvorak, J.; Jirsak, T.; Gomes, J.; Takahashi, Y.; Nakamura, K. *Phys. Rev. B* **2004**, *69*, 115414. (b) Rodriguez, J. A.; Liu, P.; Dvorak, J.; Jirsak, T.; Gomes, J.; Takahashi, Y.; Nakamura, K. *J. Chem. Phys.* **2004**, *121*, 465.

(22) Gomes, J.; Takahashi, Y.; Asakura, T.; Nakamura, K. To be published. In STM images, 90−95% of each surface examined showed a structure consistent with a Ni_3P_2 termination (Figure 1a). In general, terraces that were 600−900 Å wide were observed.

(23) St. Clair, T. P.; Oyama, S. T.; Cox, D. F.; Otani, S.; Ishizawa, Y.; Lo, R. L.; Fukui K.; Iwasawa, Y. *Surf. Sci.* **1999**, *426*, 187.

(24) Payne, M. C.; Allan, D. C.; Arias, T. A.; Johannopoulus, J. D. *Rev. Mod. Phys.* **1992**, *64*, 1045.

(25) Vanderbilt, D. *Phys. Rev. B* **1990**, *41*, 7892.

(26) Monkhorst, H. J.; Pack, J. D. *Phys. Rev. B* **1976**, *12*, 5188.

(27) Hammer, B.; Hansen, L. B.; Nørskov, J. K. *Phys. Rev. B* **1999**, *59*, 7413.

(28) Liu, P.; Rodriguez, J. A.; Muckerman, J. T.; Hrbek, J. *Phys. Rev. B* **2003**, *67*, 155416.

(29) Mulliken, R. S. *J. Chem. Phys.* **1955**, *23*, 1833.
(30) St. Clair, T. P.; Oyama, S. T.; Cox, D. F. *Surf. Sci.* **2002**, *511*, 294.
(31) Wiegand, B. C.; Uvdal, P.; Friend, C. M. *Surf. Sci.* **1992**, *279*, 105.
(32) Zaera, F.; Kollin, E. B.; Gland, J. L. *Surf. Sci.* **1987**, *184*, 75.
(33) (a) For small doses of thiophene (submonolayer coverages), the molecule desorbed from MoC in a single peak at ~190 K (heating rate in TPD 2 K/s). Assuming first-order desorption kinetics with a preexponential factor of 10^{13} s^{-1}, a Redhead analysis[33b] gives an adsorption energy of ~11 kcal/mol for thiophene on MoC. (b) Redhead, P. A. *Vacuum* **1962**, *12*, 203.
(34) Zonnevylle, M.; Hoffman, R.; Harris, S. *Surf. Sci.* **1988**, *199*, 320.
(35) Otani S.; Ishizawa, Y. *J. Cryst. Growth* **1995**, *154*, 202.
(36) Stinner, C.; Tang, Z.; Haouas, M.; Weber, T.; Prins, R. *J. Catal.* **2002**, *208*, 456.
(37) Li, S. Y.; Rodriguez, J. A.; Hrbek, J.; Huang, H. H.; Xu, G. Q. *Surf. Sci.* **1996**, *366*, 29.